Journal of the European Ceramic Society 22 (2002) 1847–1855
www.elsevier.com/locate/jeurceramsoc

Liquid-phase sintering of $Pb(Zr,Ti)O_3$ using $PbO–WO_3$ additive

E.R. Nielsen[a,*], E. Ringgaard[a], M. Kosec[b]

[a]*Ferroperm Piezoceramics A/S, Hejreskovvej 18A, DK-3490 Kvistgaard, Denmark*
[b]*Jožef Stefan Institute, Jamova 39, SI-1000 Ljubljana, Slovenia*

Received 29 August 2001; accepted 11 November 2001

Abstract

The objective of this work was to lower the sintering temperature of lead zirconate titanate (PZT) without reducing the piezoelectric performance. PZT was sintered using $PbO–WO_3$ additive of eutectic composition, which assists the densification process by liquid-phase formation. Sintering was carried out from 1075 to 1125 °C between 1 and 4 h. Density, dielectric properties and piezoelectric properties were measured. Microstructure and fracture mechanism have been studied by SEM. At the mildest sintering conditions, the additive has a positive effect on dielectric and piezoelectric properties. The liquid-phase sintering leads to a denser material without additional grain growth. PZT with $PbO–WO_3$ additive is mechanically weaker than pure PZT. The liquid phase leads to weaker grain boundaries and the material cracks in intergranular fracture, whereas pure PZT has a mixture of intergranular and transgranular fracture, and PZT sintered conventionally at 1260 °C has transgranular fracture.

Keywords: Electron microscopy; Piezoelectric properties; PZT; Sintering; Wetting

1. Introduction

The piezoelectric ceramic material $Pb(Zr,Ti)O_3$ (PZT) has many technical applications such as actuators and hydrophones. PZT is normally sintered at temperatures between 1200 and 1300 °C. For multilayer components and thick-film devices, it is desirable to bring down the sintering temperature. This will make it possible to co-fire the ceramic with internal electrodes with lower melting point, such as silver-palladium alloys,[1] or to screen-print ceramic thick films on non-refractory substrates.[2,3] Lower sintering temperatures will additionally reduce energy consumption and PbO evaporation in the process. An uncontrolled loss of PbO results in deteriorated electrical properties and is furthermore an environmental concern.

A lot of effort has been done during the last two decades to reduce the sintering temperature of PZT while retaining good piezoelectric properties. Among the methods investigated are sintering of ultra-fine powders (synthesized by chemical routes[4–7] or achieved by high-energy ball milling[8]) and liquid-phase sintering.

Many additives have been tested for liquid-phase sintering of PZT including V_2O_5,[9] $PbO–Cu_2O$,[10,11] $BiFeO_3 + Ba(Cu_{0.5}W_{0.5})O_3$,[12,13] $PbO–B_2O_3$,[14,15] $B_2O_3–Bi_2O_3–CdO$,[16–18] $Li_2CO_3–Bi_2O_3–CdCO_3$[19] and $Li_2CO_3–ZnO$.[20] Most of these studies have been focused on PZT having soft properties. The objective of this work is to reduce the sintering temperature of a hard PZT (with relative permittivity $\varepsilon_r > 1000$, mechanical quality factor $Q_m > 1000$ and loss factor tan δ below 0.4%) without degrading the properties of the ceramics.

Additives that result in a liquid-phase formation at temperatures well below the traditional sintering temperature, make it possible to achieve a dense material at reduced temperatures by liquid-phase sintering. The liquid phase speeds up the densification process by rearrangement of particles and enhanced material transport. If the constituents of the liquid can either evaporate or enter the PZT crystal lattice during the sintering, it will result in a transient liquid-phase sintering. In this case, a secondary phase between the PZT grains, reducing piezoelectric and mechanical properties, is avoided, and the end material will consist of a single phase.

In this work, a commercial type I PZT (type 100 piezoceramics according to the German DIN standard[21])

* Corresponding author. Tel.: +45-4912-7123; fax: +45-4913-8188.
E-mail address: ern@ferroperm-piezo.com (E.R. Nielsen).

0955-2219/02/$ - see front matter
PII: S0955-2219(01)00499-X

was sintered using $PbO–WO_3$ as the additive. WO_3 made up 16.5 mol% of the additive, corresponding to the eutectic composition as seen from the phase diagram in Fig. 1. Melting point of the eutectic mixture is 730 °C.[22] $PbO–WO_3$ has previously been used as an additive for sintering $Pb(Zr,Ti)O_3–Pb(Mg,Nb)O_3$ in combination with a $ZnO–Bi_2O_3$ eutectic mixture[23] and furthermore MnO_2.[24]

Kulcsar[25] finds clear donor doping effect by adding 1.5 mol% WO_3 to $Pb(Zr_{0.54}Ti_{0.46})O_3$. Recently, W has been used in compensating valence doping of PZT corresponding to following additive compositions: $Pb(W_{0.6}Li_{0.4})O_3$[26] and $Pb(Y_{2/3}W_{1/3})O_3$.[27] There has also been an intensive investigation of the $Pb(Zr_{0.53}Ti_{0.47})O_3–BiFeO_3–Ba(Cu_{0.5}W_{0.5})O_3$ system and similar systems.[13,28] Murakami et al.[13] found that WO_3 enhances grain growth.

The $PbO–WO_3$ additive is chosen for its low melting point, and for being a eutectic mixture that only introduces small amounts of new elements to the PZT material. Pb and O are already present in PZT. The new introduced element, W, is expected to enter the PZT crystal lattice. This will result in a transient liquid-phase sintering and thus to a final material that consists of one single phase. There are three general requirements for an additive for liquid-phase sintering: The liquid must be present at the sintering temperature, there must be a good wetting of the solid and there must be an appreciable solubility of the solid in the liquid.[29]

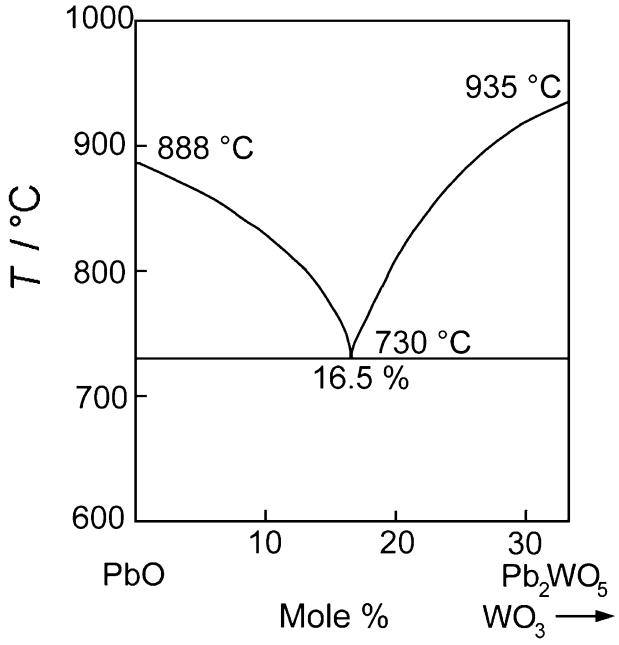

Fig. 1. Section of the $PbO–WO_3$ phase diagram.[22]

2. Experimental procedure

2.1. Sample preparation

Commercial material, Pz26, from Ferroperm Piezoceramics was used. This is a hard PZT with a composition near the morphotropic phase boundary, and the material contains several minor dopants. Three compositions were examined: "Pz26" (Pz26 with no sintering additives), "PW-p" (Pz26 powder with 1.0 wt% PbO and 0.2 wt% WO_3, corresponding to 0.3 mole% $5PbO–WO_3$, added as pure oxides) and "PW-m" (Pz26 with 1.0 wt% PbO and 0.2 wt% WO_3, where the additives were melted together previous to addition).

The sample preparation process used, involves tape casting, since one aim of the work is to produce low sinterable piezoceramic multilayer components, which are produced by tape casting. Using the same method in the development of low sinterable ceramics will make the scale-up easier.

Pz26 powder and sintering additive (in the case of PW-p and PW-m) were ball milled in toluene with a dispersing agent for 17 h. A commercial binder system was added with ball milling for an additional 2 h. The suspension was tape-cast, and the tape was stacked into blocks (thickness ≈1.4 mm). After the lamination, blocks were cut into samples of dimensions 12×24 mm, resulting in sintered dimensions of approximately 10× 20 mm. Binder was burnt out before sintering, which was carried out at 1075, 1100 and 1125 °C between 1 and 4 h with a controlled PbO atmosphere. For comparison, Pz26 was also sintered at conventional production conditions at 1260 °C. After sintering, the samples were lapped to approximately 1 mm. Silver electrodes were screen-printed onto the samples. Samples were poled in an oil bath at 130 °C using an electric field of 2.5 MV/m.

2.2. Characterisation

After lapping, samples were weighed and the dimensions were measured with micrometer for calculating geometric density. For selected samples, density was also measured by the Archimedes' method.

Dielectric properties were measured at 1 kHz with a Hewlett-Packard 4278A capacitance bridge, and piezoelectric properties were measured with a Hewlett-Packard 4194A impedance/gain-phase analyser. The d_{31} coefficient was determined from the converse piezoelectric effect by measuring displacement (mechanical TESA probe) at an electric field of 1.00 MV/m. All results presented are average values of 5 samples.

Selected samples were investigated by scanning electron microscope and EDS (Jeol JSM-5800). Both cross-sections, which were polished and chemically etched, and surfaces of fractured samples were examined. Average grain size was calculated by computer assisted image analysis using the ImageTool program.

Pz26 and PW-m sintered at 1100 °C for 2 h and conventionally sintered Pz26 were examined by powder X-ray diffraction (PXRD) using a PW3710 Philips Analytical X-ray diffractometer with CuK_α radiation. The data were collected in the 2θ-range 10–130° in steps of 0.02°. Unit cell parameters were obtained from Rietveld refinements.

2.3. Wetting experiment

To examine how well the additive wets the PZT material, some fine powder of the pre-melted eutectic mixture was placed on top of a conventionally sintered and polished Pz26 sample. This was placed in a furnace on which an optical microscope with a camera was mounted, a so-called heating-stage microscope. Profile pictures of the pile of additive powder and the sample were taken during the heating and especially during the melting of the additive. From the pictures, the contact angle between the liquid and the PZT surface was measured.

3. Results and discussion

3.1. Additive wetting of PZT

In Fig. 2, photos from the wetting experiment are shown. When the melting point of the $PbO–WO_3$ eutectic mixture is reached, the additive melts and covers the underlying PZT sample. The contact angle between the PZT surface and the liquid was approximately 10°, which means that the additive wets the PZT material excellently, which is one of the requirements for an additive for liquid-phase sintering. The melting point of the eutectic mixture is between 715 and 725 °C. Chang[22] states the melting point to be 730±5 °C.

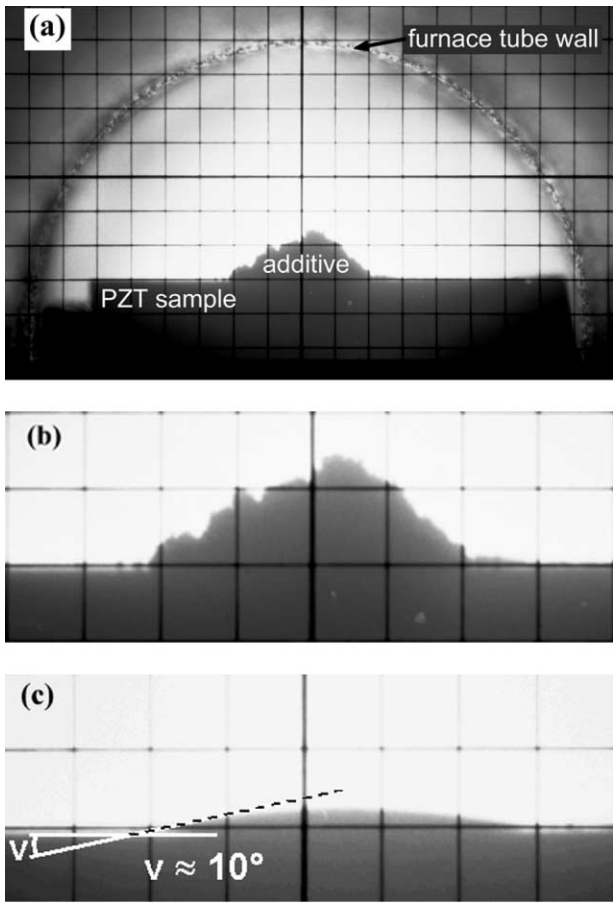

Fig. 2. Picture of wetting experiment in heating-stage microscope. $PbO–WO_3$ eutectic mixture on Pz26. (a) Experimental set-up. (b) Blow-up of section. Before melting of eutectic mixture; 715 °C. (c) Same section right after melting; 725 °C. Wetting angle: 10°.

3.2. Densification

Fig. 3 shows relative density from different sintering temperatures for PW-m and Pz26. It shows that the $PbO–WO_3$ additive helps densification of PZT. The increase in density due to the additive is more significant for the low sintering temperature and the short dwell times. At 1100 °C, 4 h, and 1125 °C, 2 and 4 h, densities close to 96% are achieved with and without the additive, whereas sintering Pz26 at 1075 °C, 1 h, results in a relative density of only 89%.

From Fig. 3, it can also be seen that when a density of approximately 96% is reached, no increase in density is achieved upon further heat treatment. Image analysis reveals smaller porosity for some of the samples, despite that holes from grains torn out during the polishing, make the apparent porosity in the image larger than it actually is in the as-sintered samples. Therefore, the geometric density was compared to density measurement by Archimedes' method for selected samples.

Archimedes' method results in negligible open porosity and approximately 3% larger densities, shifting the maximum achieved density from approximately 96 to above 99%. The explanation of this difference may be that imperfect geometric shape of samples causes an overestimation of the volume, when measuring the linear dimensions of the samples. Densities in Fig. 3 have not been corrected correspondingly, as only a few samples were measured by Archimedes' method.

Theoretical density of 7.98 g/cm^3 is calculated from the molar weight of the nominal composition of Pz26 (323.2 g/mol) and from the unit cell volume calculated from the refined PXRD data (obtained from conventionally sintered Pz26). There is some uncertainty about how well the nominal composition reflects the actual situation within the sintered material, i.e. how dopants are distributed between A- and B-sites in the perovskite structure, how much PbO has evaporated and how much segregation of second phases there is. This leads to uncertainty in the theoretical density.

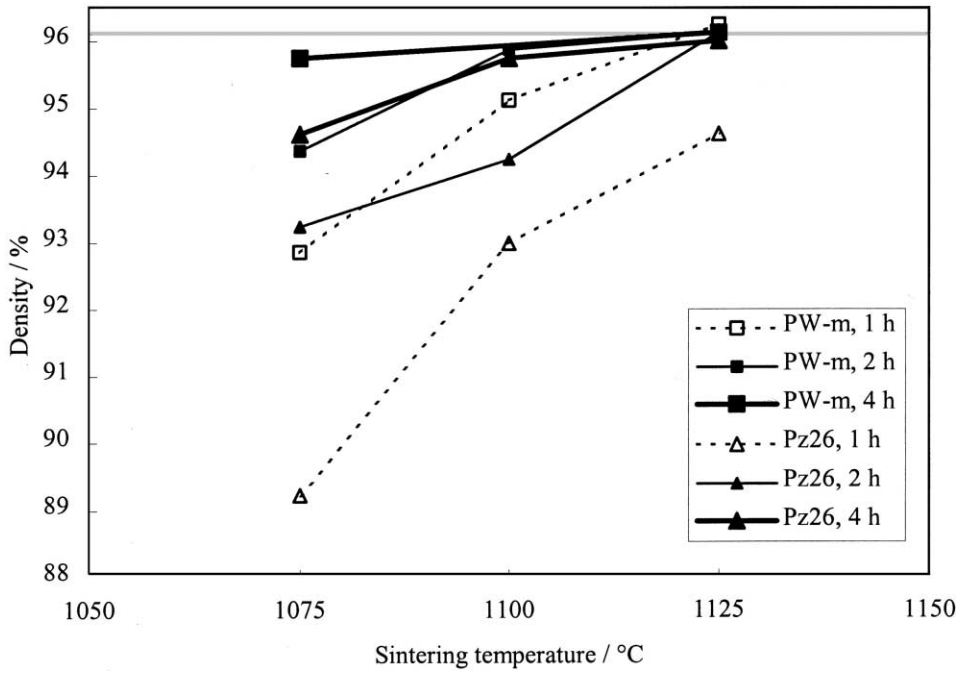

Fig. 3. Geometric density of material PW-m and Pz26 with different sintering conditions. The horizontal line in the top of the figure indicates the density of conventionally sintered Pz26 (1260 °C). Theoretical density: 7.98 g/cm^3.

3.3. Dielectric and piezoelectric properties

Relative permittivity, $\varepsilon^T_{3,r}$, for PW-m and Pz26 at the different sintering conditions is shown in Fig. 4. The PbO–WO_3 addition results in an increase in permittivity only at the mildest sintering conditions (1075 °C, 1 h). The most severe sintering conditions (1125 °C, 4 h) result in approximately the same permittivity with or without the additive. At all other conditions, the permittivity is higher for the Pz26 with no additive.

The higher density can explain the higher permittivity of PW-m at 1075 °C, 1 h. Both materials sintered at 1125 °C for 4 h have permittivities comparable to Pz26 sintered at 1260 °C. These samples also have equal densities. Although both materials sintered at 1100 °C, 2 h, almost have a density at this level, they have lower permittivity as seen in Fig. 4. It shows that even though the maximum density is achieved at 1125 °C, 2 h for Pz26, the properties improve upon further heat treatment indicating a continued development of the microstructure or chemical homogenization after 2 h.

Fig. 5 shows the relative permittivity versus density. The points representing Pz26 with and without the additive, respectively, lie on two separate lines, the Pz26 without additive having markedly higher permittivity. One might think that this is due to a change in bulk properties of the material caused by the additive. However, although the permittivity of the additive-containing samples with density below 95.5% gives a straight line, the permittivity of samples with higher density deviates from this line and almost vertically approaches the line for samples without additive, reaching comparable values. The highest permittivities for PW-p and PW-m are achieved when sintering at 1125 °C for 4 h. This indicates that when using the mild sintering conditions, additive is present as a second phase, whereas the longer sintering time and higher temperature allow the additive to enter the PZT matrix. Hence, the increase in permittivity can be explained by elimination of grain-boundary film at highest sintering temperature and longest dwell time. The low permittivities thus are results of a PZT matrix with an additive second phase having lower permittivity. Furthermore, as the samples sintered at the most severe conditions have permittivities in the same range with and without additive, it must have minor influence on the bulk permittivity, when the additive enters the PZT matrix.

Table 1 lists the dielectric loss factor, tan δ, and piezoelectric properties for PW-m and Pz26. For all three materials most of the samples have tan δ between 0.3 and 0.4%. This is also the case for conventionally sintered Pz26. Only Pz26 sintered at the mildest sintering condition (1075 °C, 1 h) shows a considerably higher tan δ of 0.7%.

The piezoelectric coupling coefficient is given as the effective coupling, k_{eff}, in the length direction. Note that effective coupling coefficients are used since the sample dimensions do not meet the required conditions for calculating k_{31} values (requirement:[21] length/width ratio >5). For PW-m, k_{eff} increases with sintering temperature and time. For Pz26, there is also an increase with time; an increase in k_{eff} with temperature is seen only at the 1-h dwell time. Maximum k_{eff} for Pz26 is achieved at

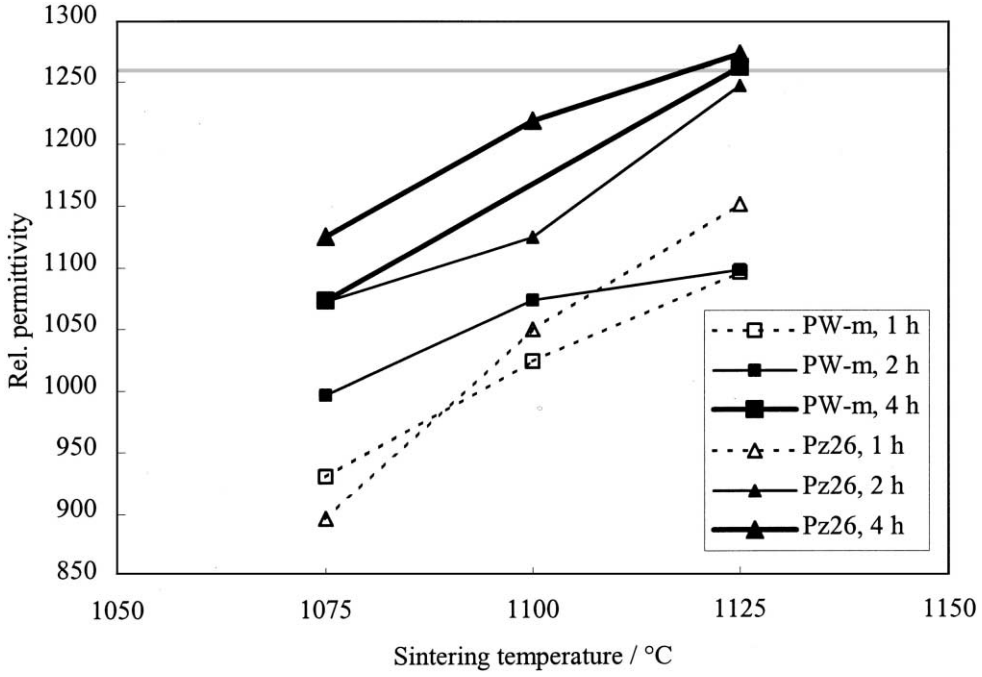

Fig. 4. Relative permittivity, $\varepsilon_{3,r}^{T}$, for PW-m and Pz26 with different sintering conditions. A typical standard deviation is 15. The horizontal line in the top of the figure indicates the permittivity level of conventional sintered Pz26 (1260 °C).

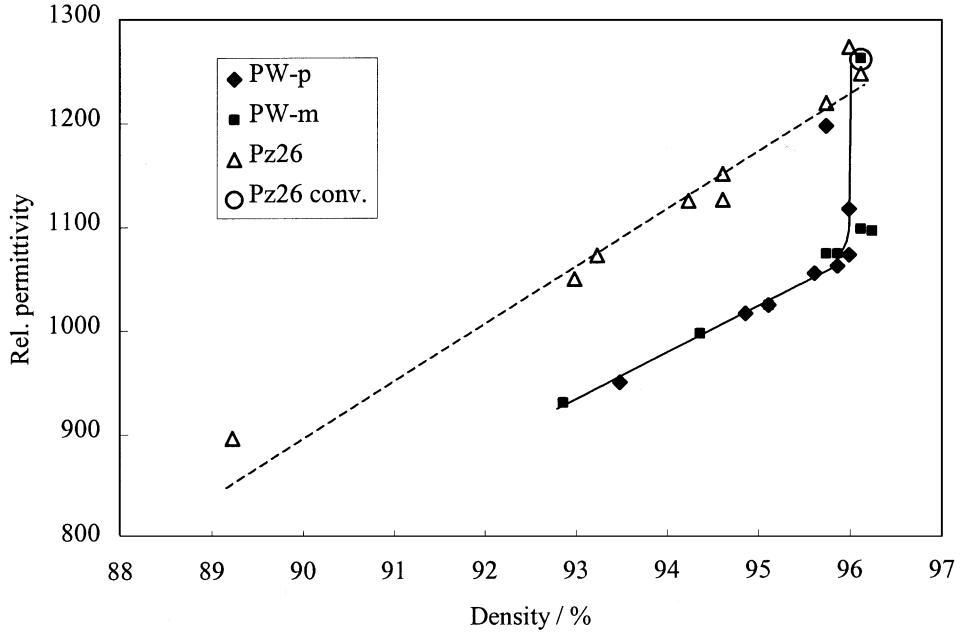

Fig. 5. Relative permittivity, $\varepsilon_{3,r}^{T}$, for PW-p, PW-m and Pz26 versus density. Each marker represents a set of sintering conditions (time and temperature) and shows the average values of 5 samples. The solid line represents samples containing PbO–WO_3 additive and the dash line represents Pz26 without additive. Properties of conventionally sintered Pz26 are marked as an open circle.

1075 °C, 4 h (26.3%). k_{eff} values of the two materials are in the same range. Most of the k_{eff} values are higher than k_{eff} of conventionally sintered Pz26.

The piezoelectric charge coefficient, $-d_{31}$, increases with sintering time and temperature. Pz26 has higher $-d_{31}$ than PW-m in all cases, except for 1125 °C, 4 h, where both Pz26 and PW-m have a d_{31} value in the same range as conventionaly sintered Pz26. Like the permittivity, d_{31} is proportionally to the density, which can explain the differences seen in d_{31} values. A similar picture is seen in the relation between d_{31} and density as in the permittivity–density relation (Fig. 5) discussed above.

The mechanical quality factor, Q_m, calculated by the impedance method[30] is also listed in Table 1. The scatter

Table 1
Dielectric loss factor, effective piezoelectric coupling coefficient (length resonance), piezoelectric charge coefficient and mechanical quality factor for PW-m and Pz26

Sintering conditions		Tan δ (%)		k_{eff} (%)		$-d_{31}$ (pC·N^{-1})		Q_m (10^3)	
		PW-m	Pz26	PW-m	Pz26	PW-m	Pz26	PW-m	Pz26
1075 °C	1 h	0.36	0.72	22.4	20.1	107	110	1.0	0.3
	2 h	0.35	0.37	23.6	24.9	117	143	0.7	0.4
	4 h	0.37	0.39	24.6	26.3	122	150	1.1	0.3
1100 °C	1 h	0.38	0.35	23.7	23.8	118	138	1.1	0.6
	2 h	0.35	0.37	24.7	24.6	126	147	1.1	0.7
	4 h	–	0.32	–	25.8	–	164	–	0.9
1125 °C	1 h	0.35	0.34	25.2	25.1	129	146	0.9	0.6
	2 h	0.45	0.34	25.5	25.3	134	160	0.9	0.8
	4 h	0.36	0.34	26.4	25.6	167	166	0.9	0.9
1260 °C		–	0.32	–	24.1	–	165	–	1.4

in Q_m values is rather large, and there is also a big variation in the standard deviations, but a typical standard variation of Q_m is $0.2{\cdot}10^3$. PW-m has higher Q_m values than Pz26. For Pz26, there is a tendency of increasing Q_m with sintering temperature. All Q_m values are below Q_m for conventionally sintered Pz26.

3.4. Powder X-ray diffraction and defect chemistry

For the samples sintered at 1100 °C for 2 h, only tetragonal PZT phase was observed, similar to the data reported for $Pb(Zr_{0.52}Ti_{0.48})O_3$.[31] If crystalline PbO or WO_3 is present in the additive-containing material, the amounts are below the detection limit. For the conventionally sintered Pz26, a small amount of ZrO_2 is additionally detected. Segregation of ZrO_2 as a second phase will slightly raise the relative Ti-content in the PZT phase.

Table 2 lists the tetragonal unit cell parameters, a and c, the unit cell volume, a^2c, and the c/a ratio, which is a measure of the tetragonal distortion of the unit cell with respect to the ideal perovskite structure. The conventionally sintered Pz26 has the smallest unit cell volume, smallest a, the largest c and hence the largest distortion. PW-m, 1100 °C, 2 h, represents the other extremes. Distortion is, thus, higher at the higher sintering temperature. This can be explained by the small increase in Ti-content of PZT upon segregation of ZrO_2 from the PZT phase, which occurs parallel to PbO vaporization that very much increases with temperature. $PbTiO_3$ has higher c/a ratio and smaller unit cell volume than PZT,[31,32] and a higher Ti-content in PZT shifts the unit cell parameters towards those of $PbTiO_3$.

Table 2
Tetragonal unit cell parameters, volume and tetragonal distortion obtained from Rietveld refinement of PXRD data. The number in parenthesis is the estimated standard deviation of cell parameters

	a(Å)	c(Å)	a^2c(Å^3)	c/a
PW-m, 1100 °C, 2 h	4.0466 (2)	4.1155 (3)	67.39	1.0170
Pz26, 1100 °C, 2 h	4.0428 (2)	4.1215 (3)	67.36	1.0195
Pz26, 1260 °C	4.03795 (7)	4.1262 (1)	67.28	1.0219

Ionic radii for the additive elements and the PZT elements are given in Table 3 for the coordination numbers (CN) of relevance (from Shannon [33]). When the additive enters the PZT crystal lattice during sintering, W is expected to enter the B-site of the ABO_3 perovskite structure as W^{6+}, whereas Pb^{2+} naturally is expected to enter the A-site.

The defect chemistry of Pz26 is quite complex as it, besides the $Pb(Zr,Ti)O_3$ and the possible PbO evaporation, consists of several dopants and in the present experiments furthermore an additive. Excess PbO from the additive, may suppress the PbO vaporization from the PZT matrix and result in fewer vacancies. Replacing Zr^{4+} and Ti^{4+} with W^{6+} is so-called donor doping, which normally results in cation vacancies leading to soft properties. We do not see clear donor doping effects by the additive. That may be because of the relatively small amount of additive (0.3 mol%), but it can also be due to another possible charge-compensation mechanism in Pz26: Besides lead zirconate titanate, Pz26 contains small amounts of dopants that are able to show

Table 3
Ionic radii for the elements in PZT and additive elements.[33] CN is the coordination number of the different sites in the ABO_3 perovskite structure

	Ion	Ionic radius (Å)
A-site (CN: 12)	Pb^{2+}	1.49
B-site (CN: 6)	Zr^{4+}	0.72
	Ti^{4+}	0.605
	W^{6+}	0.6
O-site (CN: 6)	O^{2-}	1.40

various oxidation states; therefore, charge compensation may occur by reduction of dopant elements. Whereas vacancies will make the crystal lattice shrink and thus result in a smaller unit cell volume, a reduction of dopant elements will lead to larger ionic radii and thus result in a larger unit cell.

That higher sintering temperature for PZT leads to smaller unit cell volume can be explained by a combination of Pb-vacancies and higher Ti-content, which comes from the PbO vaporization followed by segregation of ZrO_2 as described above. The decrease in unit cell volume with sintering temperature seen here, is different from some other findings.[34,35]

One might think that W^{6+} cannot be charge-compensated by cation-vacancy formation, as we see a slight increase in the unit cell volume when using PbO–WO_3 additive. The simultaneous addition of PbO can nevertheless counteract the contraction of the unit cell, as it will suppress vaporization of PbO from the PZT matrix and hence lead to fewer vacancies and prevent ZrO_2 segregation. Therefore, we cannot exclude the possibility of cation vacancy formation by the W^{6+} addition, but the increase in unit cell volume and the lack of softening of properties upon W^{6+} addition, make reduction of dopant elements more likely.

The largest amount of W^{6+} is expected to enter the crystal lattice at the most severe sintering conditions. As the samples sintered at these conditions have comparable properties with and without additive, it can be concluded that the change in the defect chemistry by introducing W^{6+} in the PZT lattice does not affect the electrical properties of the material significantly, at least not in the amount used here.

3.5. Microstructure

All samples examined by SEM have a uniform microstructure. In some of the samples, small segregations of ZrO_2 are seen as a second phase, mostly in connection with pores. The amount of ZrO_2 and the size of the segregations increase with the sintering temperature, and ZrO_2 segregation is more pronounced in samples with no additive. This confirms the hypothesis that ZrO_2 segregation is due to the vaporization of PbO. Fig. 6 shows SEM micrographs of PW-m and Pz26 sintered at 1125 °C for 2 h. The additive-containing materials PW-p and PW-m have slightly smaller grain size than Pz26 (see Table 4). This means that the liquid phase leads to a more dense material without additional grain growth. When the additive melts, the formed liquid wets and covers each grain by a liquid film, which works as a grain growth inhibitor. When a liquid shows good wetting of a grain, it is because formation of the liquid film results in reduced interface energy. The driving force for grain growth is thus lowered. Furthermore, the process of solution, diffusion through a liquid film and precipitation, is usually slower than the jump across a grain boundary.[36] Some studies of liquid-phase sintering of PZT, however, find that the additive works as a grain growth promoter.[15] The effect of liquid phase on grain growth must be dependent on the liquid used, according to the solubility of PZT in the liquid and the liquid wetting of PZT.

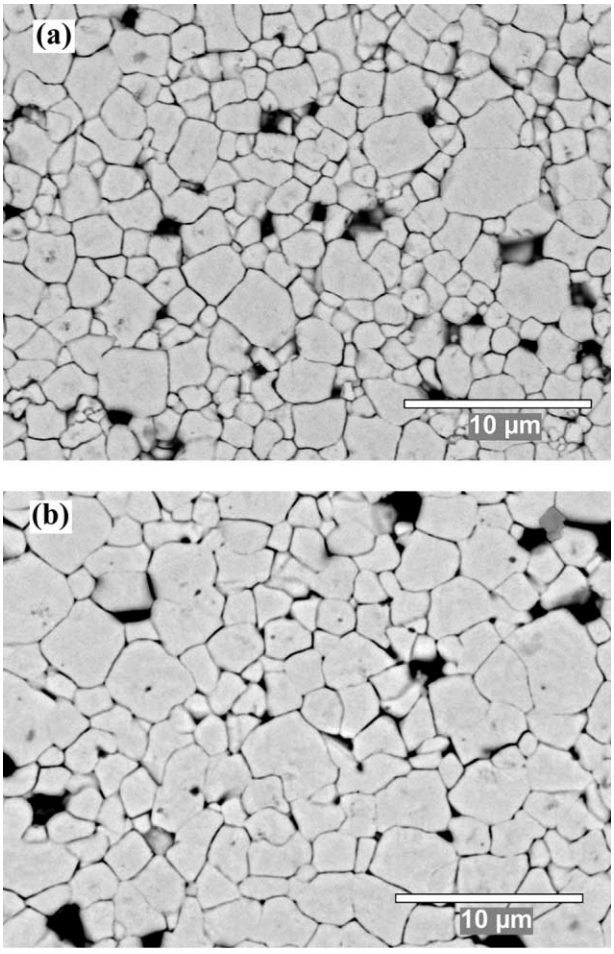

Fig. 6. SEM micrographs of polished and etched samples. (a) PW-m sintered at 1125 °C, 2 h. (b) Pz26 sintered at 1125 °C, 2 h; in the top right corner, small segregations of ZrO_2 are seen.

Table 4
Grain size of PW-p, PW-m and Pz26. Average Feret diameter in μm

	Pz26	PW-m	PW-p
1075 °C, 2 h	1.5	1.1	
1100 °C, 2 h	1.8	1.4	1.1
1125 °C, 2 h	1.8	1.2	
1260 °C	4.1		

Samples containing sintering additive were very easily etched in acid to reveal grain boundaries, and the samples were also easily broken for fracture studies. Fracture surfaces of PW-m (1125 °C, 2 h) and Pz26 (1125 °C, 2 h and 1260 °C) are shown in Fig. 7. PW-m clearly has

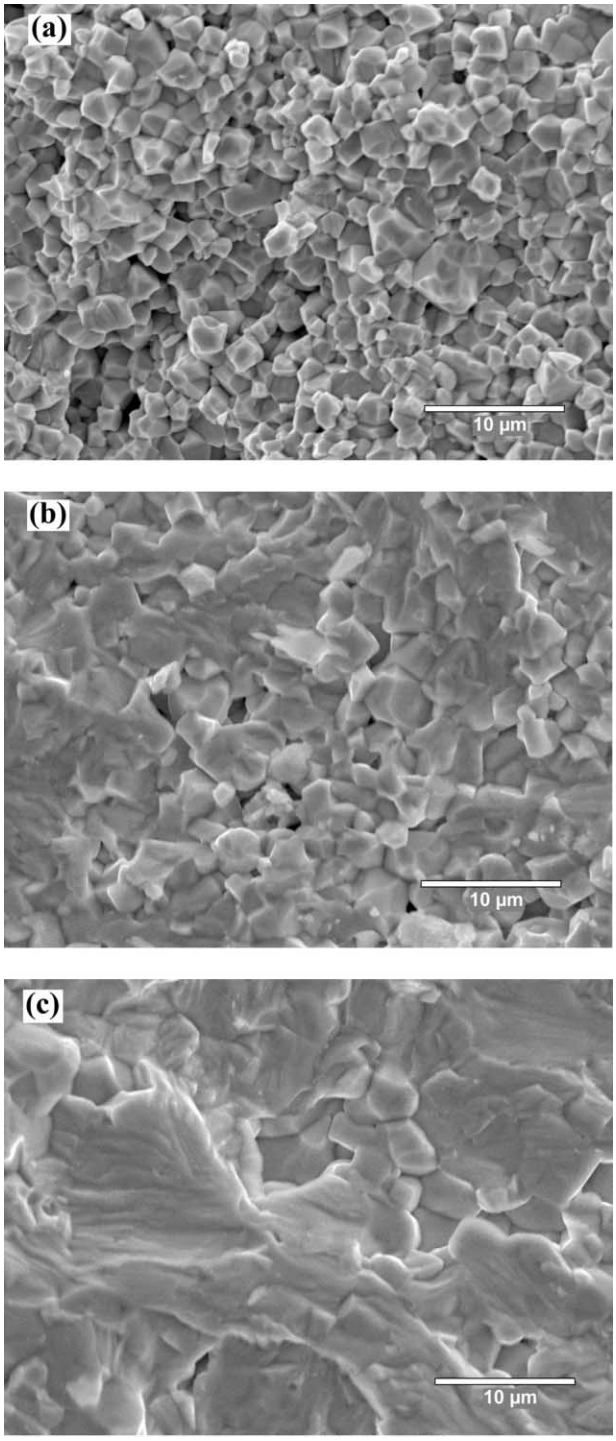

Fig. 7. Scanning micrographs of fracture surface of (a) PW-m, 1125 °C, 2 h, (b) Pz26, 1125 °C, 2 h and (c) Pz26 sintered at 1260 °C.

an intergranular fracture mechanism [Fig. 7(a)] indicating that the grain boundaries are mechanically weaker than the grains. This was the same for all additive-containing samples that were examined. Pz26 sintered at the low temperatures, shows a mixture of intergranular and transgranular fracture [Fig. 7(b)], indicating that grains and boundaries have approximately same strength, whereas Pz26 sintered at 1260 °C breaks with transgranular fracture [Fig. 7(c)]. Thus, the sintering additive causes a change in the grain boundary properties. Whether the PbO and WO_3 or only one of the additive constituents is present at the grain boundaries, as glass phase or crystalline secondary phase, is not known. No secondary phases have been identified by SEM or EDS. Nevertheless, it is believed that part of the sintering additive is present at the grain boundaries in small amounts.

Table 5
Properties of PZT with PbO–WO_3 added as pure oxides (PW-p) and melted together (PW-m). Sintering conditions: 1100 °C, 2 h

	Rel. density (%)	$\varepsilon^T_{3,r}/10^3$	tan δ (%)	k_{eff} (%)	$-d_{31}$ (pC·N^{-1})	Q_m (10^3)
PW-p	95.9	1.06	0.35	23.9	122	1.0
PW-m	95.9	1.07	0.35	24.7	126	1.1

3.6. Effect of pre-melting the additive

The pre-melted additive results in slightly better properties than the pure oxide additive. PW-m has a higher k_{eff} than PW-p, but most of the other differences are within the standard deviations. In Table 5, properties for PW-p and PW-m sintered at 1100 °C for 2 h are listed.

4. Conclusions

Lead zirconate titanate (PZT) has been sintered at temperatures between 1075 and 1125 °C using the PbO–WO_3 additive. The additive shows excellent wetting of PZT. The eutectic mixture assists densification without additional grain growth.

When sintering at 1075 °C for 1 h, the additive has a significant positive effect on dielectric and piezoelectric properties. At other sintering conditions, the additive leads to slightly improved coupling coefficient, improved mechanical quality factor, Q_m, reduced $-d_{31}$ and reduced permittivity. Sintering PZT with or without additive for 4 h at 1125 °C results in properties comparable to conventionally sintered PZT except for a reduced Q_m.

The additive results in mechanically weaker grain boundaries, which can be seen by the intergranular fracture mechanism, whereas PZT without additive has transgranular fracture mechanism or a mixture of the two fracture mechanisms.

Whether the eutectic mixture was melted together before adding to the PZT powder or was added as

pure oxides, only caused a minor difference in final properties.

Acknowledgements

Thanks to Dr. D. Kuščer (Jožef Stefan Institute, Slovenia), for help with SEM examinations, Dr. B. Malič (Jožef Stefan Institute, Slovenia), Dr. F.W. Poulsen (Risø National Laboratory, Denmark) and Dr. K. Ståhl (Technical University of Denmark) for fruitful discussions and Dr. K. Ståhl also for help with PXRD.

References

1. Wersing, W., Wahl, H. and Schnöller, M., PZT-based multilayer piezoelectric ceramics with AgPd-internal electrodes. *Ferroelectrics*, 1988, **87**, 271–294.
2. Wolny, W.W., Piezoelectric thick films—technology and applications. State of the art in Europe. In *ISAF 2000. Proceedings of the 2000 12th IEEE International Symposium on Applications of Ferroelectrics*. Honolulu, Hawaii, USA, July 21–August 2, 2000, ed. S. K. Streiffer, B. J. Gibbons and T. Tsurumi, 2000, 257–261.
3. Schönecker, A., Gesemann, H.-J. and Seffner, L., Low-sintering PZT-ceramics for advanced actuators. In *ISAF '96. Proc. of the Tenth IEEE International Symposium on Applications of Ferroelectrics*, Vol. 1, ed. B.M. Kulwicki, A.A. Amin and A. Safari. 1996, pp. 263-266.
4. Kosec, M. and Malič, B., Sol-gel synthesis and sintering of PZT based powders. In *Fourth ECerS. Proc.4th European Ceramic Society Conf. Vol.5. Electroceramics*, ed. G. Gusmano and E. Traversa. Gruppo editoriale Faenza Editrice, Faenza, 1995, pp. 9–16.
5. Saegusa, K., Preparation by a sol-gel process and dielectric properties of lead zirconate titanate glass-ceramic thin films. *Jpn. J. Appl. Phys*., 1997, **36**, 3602–3608.
6. Tomandl, G., Stiegelschmitt, A. and Böhner, R., Lowering the sintering temperature of PZT-ceramic by sol-gel processing. *Science of Ceramics*, 1988, **14**, 305–308.
7. Lozano, J. F. F., Duran, P. and Moure, C., Low sintering temperature of Nb-doped PZT obtained by using oxalate precursors. *Science of Ceramics*, 1988, **14**, 897–902.
8. Kong, L. B., Ma, J., Zhu, W. and Tan, O. K., Reaction sintering of partially reacted system for PZT ceramics via a high-energy ball milling. *Scripta Mater*., 2001, **44**, 345–350.
9. Wittmer, D. E. and Buchanan, R. C., Low-temperature densification of lead zirconate–titanate with vanadium pentoxide additive. *J. Am. Ceram. Soc*., 1981, **64**, 485–490.
10. Corker, D. L., Whatmore, R. W., Ringgaard, E. and Wolny, W. W., Liquid-phase sintering of PZT ceramics. *J. Eur. Ceram. Soc*., 2000, **20**, 2039–2045.
11. Ringgaard, E., Nielsen, E.R. and Wolny, W.W., Optimisation of new liquid-phase sintering aid for PZT. In *ISAF 2000. Proceedings of the 2000 12th IEEE International Symposium on Applications of Ferroelectrics*. Honolulu, Hawaii, USA, July 21–August 2, 2000, ed. S. K. Streiffer, B. J. Gibbons and T. Tsurumi, 2000, 451–454.
12. Kaneko, S., Dong, D. and Murakami, K., Effect of simultaneous addition of $BiFeO_3$ and $Ba(Cu_{0.5}W_{0.5})O_3$ on lowering of sintering temperature of $Pb(Zr,Ti)O_3$ Ceramics. *J. Am. Ceram. Soc*., 1998, **81**, 1013–1018.
13. Murakami, K., Mabuchi, D., Kurita, T., Niwa, Y. and Kaneko, S., Effects of adding various metal oxides on low-temperature sintered $Pb(Zr,Ti)O_3$ ceramics. *Jpn. J. Appl. Phys*., 1996, **35**, 5188–5191.
14. Tandon, R. P., Singh, V., Narayanaswami, N. and Hans, V. K., Low temperature sintering of PZT ceramics using a glass additive. *Ferroelectrics*, 1997, **196**, 117–120.
15. Wang, C.-H. and Wu, L., $4PbO–B_2O_3$—a new sintering agent for $Pb(Zr,Ti)O_3$ ceramics. *Jpn. J. Appl. Phys*., 1993, **32**, 3209–3213.
16. Gui Zhilun, Li Longtu, Gao Suhua and Zhang Xiaowen, Low-temperature sintering of lead-based piezoelectric ceramics. *J. Am. Ceram. Soc*., 1989, **72**, 486–491.
17. Li Longtu, Zhang Xiaowen and Chai Jinghe, Low temperature sintering of PZT ceramics. *Ferroelectrics*, 1990, **101**, 101–108.
18. Tandon, R. P., Singh, V. and Singh, R., Properties of Low temperature sintered neodymium doped lead zirconate titanate ceramics. *J. Mater. Sci. Lett*., 1994, **13**, 810–812.
19. Wang, X., Murakami, K. and Kaneko, S., High-performance $PbZn_{1/3}Sb_{2/3}O_3–PbNi_{1/2}Te_{1/2}O_3–PbZrO_3–PbTiO_3$ ceramics sintered at a low temperature with the aid of complex additives $Li_2CO_3–Bi_2O_3–CdCO_3$. *Jpn. J. Appl. Phys*., 2000, **39**, 5556–5559.
20. Gui, Z., Hu, H., Li, L. and Zhang, X., Influence of additives on sintering processing and properties of high performance piezoelectric ceramics. *Solid State Phenomena*, 1992, **25**&**26**, 309–316.
21. Deutsche Norm, *DIN VDE 0336-1*, 1999.
22. Chang, L. L. Y., Phase relations in the system $PbO–WO_3$. *J. Am. Ceram. Soc*., 1971, **54**, 357.
23. Gesemann, H.-J. and Schönecker, A., Low sintering PZT by liquid phase formation. In *Electroceramics IV, Vol. 2*, ed. R. Waser. Verlag der Augustinus, Buchhandlung, 1994, pp. 1259–1262.
24. Gesemann, R. and Gesemann, H.-J., Niedrig sinternde PZT-Versätze. German patent DE 41 27 829 A1, 4 March 1993.
25. Kulcsar, F., Electromechanical Properties of lead titanate zirconate ceramics modified with tungsten and thorium. *J. Am. Ceram. Soc*., 1965, **48**, 54.
26. Dimitriu, E., Ramer, R., Miclea, C. and Tanasoiu, C., Piezoelectric properties of tungsten doped PZT type materials. *Ferroelectrics*, 2000, **241**, 1851–1857.
27. Seok-Jin Yoon, Hyun-Jai Kim, Hyung-Jin Jung and Chang-Yub Park, Dielectric and piezoelectric properties of $xPb(Y_{2/3}W_{1/3})O_3–(1-x)\ Pb(Zr_{0.52}Ti_{0.48})O_3$ ceramics. *Ferroelectrics*, 1993, **145**, 1–7.
28. Sheng-Yuan Chu and Cheng-Shung Hsieh, Doping effects on the piezoelectric properties of low-temperature sintered PNN–PZT-based ceramics. *J. Mater. Sci. Lett*., 2000, **19**, 609–612.
29. Kwon, O.-H., Liquid-phase sintering. In *Ceramics and Glasses, Engineered Materials Handbook,* Vol 4, ed. S. J. Schneider, 1991, pp. 285–290.
30. Deutsche Norm, *DIN VDE 0336-2*, 1999.
31. Kakegawa, K., Mohri, J., Takahashi, T., Yamamura, H. and Shirasaki, S., A compositional fluctuation and properties of $Pb(Zr,Ti)O_3$. *Solid State Commun*., 1977, **24**, 769–772.
32. Nelmes, R. J. and Kuhs, W. F., The crystal structure of tetragonal $PbTiO_3$ at room temperature and at 700 K. *Solid State Comm*., 1985, **54**, 721–723.
33. Shannon, R. D., Revised effective ionic radii and systematic studies of interatomic distances in halides and chalcognides. *Acta Cryst*., 1976, **A32**, 751.
34. Lucuta, P. G., Constantinescu, F. and Barb, D., Structural dependence on sintering temperature of lead zirconate–titanate solid solutions. *J. Am. Ceram. Soc*., 1985, **68**, 533–537.
35. Boutarfaia, A., Investigations of co-existence region in lead zirconate-titanate solid solutions, X-ray diffraction studies. *Ceram. Int*., 2000, **26**, 583–587.
36. Kingery, W. D., Bowen, H. K. and Uhlmann, D. R., *Introduction to Ceramics*, 2nd edn. John Wiley & Sons, New York, 1976.